

XTQA: Span-Level Explanations of the Textbook Question Answering

Jie Ma^{1,2}, Jun Liu^{1,2}, Junjun Li^{2,3}, Qinghua Zheng^{1,2}, Qingyu Yin⁴, Jianlong Zhou⁵, Yi Huang⁶

¹National Engineering Lab for Big Data Analytics, Xi'an Jiaotong University, Xi'an, Shaanxi 710049, China

²School of Computer Science and Technology, Xi'an Jiaotong University

³Shaanxi Province Key Laboratory of Satellite and Terrestrial Network Tech. R&D, Xi'an Jiaotong University

⁴ Amazon.com Inc

⁵Department of Computer Science, Xi'an Jiaotong University City College, Xi'an 710018, China

⁶China Mobile Research, Beijing 100032, China

Abstract

Textbook Question Answering (TQA) is a task that one should answer a diagram/non-diagram question given a large multi-modal context consisting of abundant essays and diagrams. We argue that the explainability of this task should place students as a key aspect to be considered. To address this issue, we devise a novel architecture towards span-level explanations of the TQA (XTQA). It can provide not only the answers but also the span-level evidences to choose them for students based on our proposed coarse-to-fine grained algorithm. The algorithm first coarsely chooses top M paragraphs relevant to questions using the TF-IDF method, and then chooses top K evidence spans finely from all candidate spans within these paragraphs by computing the information gain of each span to questions. Experimental results show that our method significantly improves the state-of-the-art performance compared with baselines. The source code is available at <https://github.com/keep-smile-001/opentqa>.

1 Introduction

Question Answering (QA) has attracted extensive interest in the fields of Computer Vision (CV) and Natural Language Processing, such as Visual Question Answering (VQA) (Yu et al., 2019; Khademi, 2020) in CV and Machine Reading Comprehension (MRC) (Nie et al., 2019; Saxena et al., 2020) in NLP. Recently, a new task named Textbook Question Answering (TQA) (Kembhavi et al., 2017) that aims to answer diagram/non-diagram questions given a large multi-modal context consisting of diagrams, text and few natural images was proposed. The task is developed from middle school science curricula and describes the real-life process of a student who learns new knowledge from books and assesses learning achievement. Compared with

MRC and VQA, TQA is more complex and more realistic.

In real-life scenarios, the TQA robot should not only answer a question accurately, but also give *students* the reason to choose the answer. Although existing neural-symbolic works (Yi et al., 2018; Mao et al., 2019) on the CLEVR dataset make significant progress on the explainability, they are not applicable to the TQA dataset. Here are two reasons for this. First, the curriculum is diverse in the TQA dataset, which makes the design of the domain-specific language (DSL) difficult. Second, there is no any supervision information except the answer label.

An analysis (Kembhavi et al., 2017) of the information scope required to answer questions in the TQA dataset shows that about 80% of the questions require a single sentence or multiple sentences. Inspired by this, we may be able to provide the evidence spans¹ about questions for students, which would give them explainability to some extent. For example, when the TQA robot gives students the correct answer B to the question 1 , it also provides an evidence span as the explanation in Figure 1. We make an assumption owing to the lack of supervision information of evidence spans in the TQA dataset. **Assumption: if a question is answered accurately after fusing a generated span and other essential information, the span is a gold evidence to the question.** For example, the span marked in green in the middle part of Figure 1 is a gold evidence to the question 1 .

Based on the assumption, we devise a novel architecture towards span-level explanations of the Textbook Question Answering (XTQA) as illustrated in Figure 1. First, XTQA uses our proposed coarse-to-fine grained algorithm to generate evidence spans of questions. In the coarse grained

¹In this paper, spans are represented by the indexes of sentences instead of words.

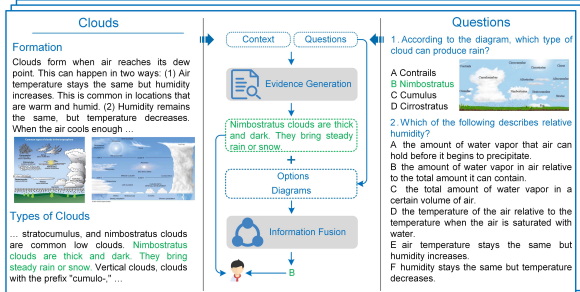


Figure 1: An example of the TQA task and a brief illustration of our work. The abundant essays and diagrams of a lesson are shown in the left part. The diagram/non-diagram questions of this lesson are shown in the right part.

phase, top M paragraphs relevant to questions are chosen from abundant essays by the TF-IDF score. In the fine grained phase, top K evidence spans are generated from all candidate spans within the top M paragraphs by computing the information gain of each span to questions. The larger information gain indicates the more uncertainty of questions reduced by spans. Second, XTQA fuses the information of generated evidence spans, questions, options and diagrams to provide answers. Finally, not only the answers but also the evidences to choose them are provided to students.

The contributions of our work are as follows. (1) We devise a novel architecture that can give students evidences as well as answers for TQA. (2) We propose a coarse-to-fine grained algorithm to generate span-level evidences by computing the information gain of each span to questions. (3) We conduct extensive experiments and ablation studies on the TQA dataset (Kembhavi et al., 2017) to verify the effectiveness of the XTQA and our proposed assumption. Experimental results show that XTQA significantly improves the state-of-the-art performance compared with baselines. (4) We also explore how to effectively integrate the self-supervised learning method SimCLR (Chen et al., 2020) into the proposed architecture to further improve the accuracy of the TQA task.

2 Related Work

Since the TQA task is similar to MRC and VQA, we briefly review some of their research relevant to our work.

MRC requires a machine to answer questions accurately given a textual context (Lehnert, 1977). Wang et al. (2018) proposed a multi-granularity hi-

erarchical attention fusion network to answer questions for a given narrative paragraph. Lee et al. (2018) proposed a paragraph ranker to improve the answer recall with less noise. Ding et al. (2019) proposed CogQA that builds a cognitive graph by an implicit extraction module and an explicit reasoning module to address the multi-hop question answering. Although the above studies achieved success, they did not estimate the relationship and combined design of retrieval and comprehension. Nie et al. (2019) proposed a hierarchical pipeline model that reveals the importance of semantic retrieval to give general guidelines on the system design for MRC.

Unlike the MRC task, the TQA task not only involves the textual question but also the visual question. In this paper, we first apply the self-supervised learning method SimCLR (Chen et al., 2020) to learn the diagram representation in the TQA dataset to the best of our knowledge.

VQA requires a machine to answer questions accurately given an image (Antol et al., 2015). Yang et al. (2016) proposed stacked attention networks that perform multi-step reasoning to infer answers. Kim et al. (2017) proposed a low-rank bi-linear pooling method using Hadamard product to address the complex computation. However, the above methods consider little on the effectiveness of the explicit regions for answering. To address this issue, Anderson et al. (2018) proposed a combined bottom-up and top-down attention mechanism that computes attentions at the level of salient image regions and objects. Gao et al. (2019) proposed a multi-modality latent interaction module to model the summarization of language and visual information. However, these methods may not perform complex reasoning. To address this issue, Yi et al. (2018) proposed a neural-symbolic visual question answering architecture that disentangles question and image understanding from reasoning. Based on this paper, Mao et al. (2019) proposed a neuro-symbolic reasoning module that executes generated programs on the latent scene representations to perform reasoning. These methods can execute complex logic reasoning based on the manually designed domain-specific language.

Unlike the VQA task, the TQA task contains multi-modal context except questions and diagrams. In this paper, we argue that the explainability of the TQA task should place *students* as a key aspect to be considered. We propose a coarse-to-fine

grained algorithm to provide the evidence spans of questions for students.

3 Task Formulation

The TQA dataset contains two types of questions: diagram questions and non-diagram questions. Therefore, the TQA task can be classified into two categories: diagram question answering and non-diagram question answering. Owing to the difference only at this point between them, here we give the task formulation of the diagram question answering.

Given a dataset \mathcal{S} consisting of n triplets $(c_i, d_i, q_i, \mathcal{A}_i)$ with $c_i \in \mathcal{C}$ representing multi-modal context of a lesson, $d_i \in \mathcal{D}$ representing a diagram, $q_i \in \mathcal{Q}$ representing a question and $\mathcal{A}_i \subseteq \mathcal{A}$ representing the candidate answers of q_i , one must optimize the parameters θ of the function $f : \mathcal{C} \times \mathcal{D} \times \mathcal{Q} \rightarrow \mathbb{R}^{|\mathcal{A}|}$ to produce accurate predictions. $a_{i,j} \in \mathcal{A}_i$ denotes the j -th candidate answer of q_i .

A candidate evidence span $e_{i,k} \in \mathcal{E}_i \subseteq \mathcal{E}$ to q_i is represented by its start $\text{START}(k)$ and end $\text{END}(k)$ indexes respectively following (Ma et al., 2020), where \mathcal{E}_i represents the candidate evidence span set of q_i , $1 \leq k \leq N$, $1 \leq \text{START}(k) \leq \text{END}(k) \leq t$ and $N = \frac{t(t+1)}{2}$ is the number of candidate evidence spans supposing c_i containing t sentences. We rewrite the function $f : \mathcal{E} \times \mathcal{D} \times \mathcal{Q} \rightarrow \mathbb{R}^{|\mathcal{A}|}$ since evidence spans and other essential information are fused to answer questions. To summarize, we optimize θ to obtain not only the correct answer a_i but also the evidence span e_i to q_i based on the assumption in Section 1.

4 Method

The architecture of the XTQA is shown in Figure 2. It consists of four modules: question/answer representation, evidence span generation, diagram representation and answer prediction.

Question/Answer representation. This module uses GRUs and learned attention mechanisms to obtain the word-level representations $q'_i/a'_{i,j}$ and global representations $q''_i/a''_{i,j}$ of the question/candidate answer $q_i/a_{i,j}$ respectively.

Evidence span generation. This module uses our proposed coarse-to-fine grained algorithm to obtain the representations e''_i of the top K evidence spans to q_i and their indexes $[\text{START}(k), \text{END}(k)]$ from all candidate spans within top M paragraphs p_i .

Diagram representation. This module uses CNNs to obtain the representation d'_i of the diagram d_i .

Answer prediction. This module gives students not only the predicted answer \hat{a}_i but also the evidence span e_i to choose it after multi-modal information fusing.

4.1 Question/Answer Representation

We use uni-directional GRUs to obtain the d_1 -dimensional word-level representations $q'_i \in \mathbb{R}^{X \times d_1}$ and $a'_{i,j} \in \mathbb{R}^{Y \times d_1}$ of q_i and $a_{i,j}$ respectively as follows:

$$\begin{aligned} q'_i &= \text{GRU}_s(\text{embedding}(q_i)), \\ a'_{i,j} &= \text{GRU}_s(\text{embedding}(a_{i,j})), \end{aligned} \quad (1)$$

where $q_i \in \mathbb{R}^{X \times 1}$ denotes the i -th question, $a_{i,j} \in \mathbb{R}^{Y \times 1}$ denotes the j -th candidate answer of q_i , X and Y denotes the maximum length of q_i and $a_{i,j}$ respectively, and $\text{embedding}(\cdot)$ is used to get word embeddings.

We use learned attention mechanisms to obtain the d_1 -dimensional global information $q''_i \in \mathbb{R}^{d_1 \times 1}$ and $a''_{i,j} \in \mathbb{R}^{d_1 \times 1}$ of q_i and $a_{i,j}$ respectively as follows:

$$\begin{aligned} \alpha &= \text{softmax}(\text{MLP}_s(q'_i)), \\ q''_i &= \sum_{u=1}^X \alpha_u \circ q'_{i,u}, \end{aligned} \quad (2)$$

where $\alpha \in \mathbb{R}^{X \times 1}$ is the learned attention weight matrix by MLPs, \circ denotes the element-wise product, and $q'_{i,u}$ is the u -th word representations of q_i . $a''_{i,j}$ is obtained by analogy.

4.2 Evidence Span Generation

Although the multi-modal context c_i contains abundant essays, only a single sentence or multiple sentences would be required to answer q_i . Inspired by this, we propose a coarse-to-fine grained algorithm to generate evidence spans of q_i .

In the coarse phase, the TF-IDF method is used to narrow down the scope of textual context from a lesson to top M paragraphs p_i relevant to q_i . $p_i \in \mathbb{R}^{M \times L \times O}$ can be denoted as follows:

$$p_i = \text{TFIDF}(q_i, c_i), \quad (3)$$

where L is the maximum number of sentences in each paragraph, and O is the maximum length of each sentence. The shared GRU_s in Equation 1 is

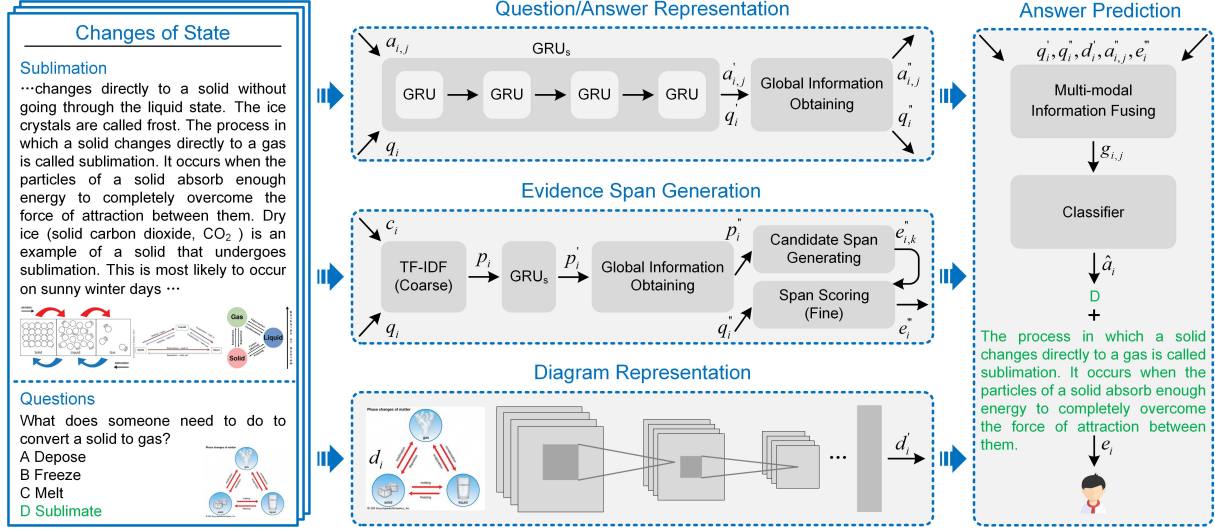


Figure 2: The architecture towards span-level eXplanations of the Textbook Question Answering (XTQA). The left part shows a lesson and a question in the TQA dataset. The index of the evidence span to a question is obtained by our proposed coarse-to-fine grained algorithm in the middle module of the middle part.

used to obtain the d_1 -dimensional word-level representation $p_i' \in \mathbb{R}^{M \times L \times O \times d_1}$ of p_i . We also use the shared learned attention mechanism in Equation 2 to obtain the d_1 -dimensional global representations $p_i'' \in \mathbb{R}^{M \times L \times d_1}$ of sentences within p_i .

Algorithm 1: Evidence span generation

Input: question q_i , multi-modal context c_i .

Output: representation e_i'' of evidence span e_i and its index.

- 1 Choose top M paragraphs using Equation 3;
- 2 Obtain the whole candidate evidence span representations according to their indexes using Equation 4;
- 3 Compute the information gain of each span to q_i using Equation 6;
- 4 Choose top K evidence span.

In the fine-grained phase, top K evidence spans are generated from all candidate spans within top M paragraphs by computing the information gain of each span to questions. Concretely, the representation at the $\text{START}(k)$ and $\text{END}(k)$ index as described formally in Section 3 are concatenated to generate the candidate evidence span representation $e_{i,k}' \in \mathbb{R}^{M \times N \times 2d_1}$ as follows:

$$e_{i,k}' = [p_{i,\text{START}(k)}''; p_{i,\text{END}(k)}''], \quad (4)$$

where $N = \frac{L(L+1)}{2}$ is the number of candidate evidence spans within each paragraph. To obtain the final candidate evidence span representation

$e_{i,k}'' \in \mathbb{R}^{M \times N \times d_1}$, we apply the average pooling AP with kernel size 2 on $e_{i,k}'$ as follows:

$$e_{i,k}'' = \text{AP}(e_{i,k}'). \quad (5)$$

We compute the information gain $g(q_i, e_{i,k})$ of each candidate evidence span $e_{i,k}$ to the question q_i for obtaining the top K evidence span. $g(q_i, e_{i,k})$ can be denoted as follows:

$$g(q_i, e_{i,k}) = H(q_i) - H(q_i|e_{i,k}), \quad (6)$$

where $H(q_i)$ is the entropy of q_i , i.e., the uncertainty of q_i , and $H(q_i|e_{i,k})$ is the conditional entropy of q_i given $e_{i,k}$, i.e., the uncertainty of q_i given $e_{i,k}$. The larger information gain indicates the more uncertainty of q_i reduced by $e_{i,k}$. $H(q_i)$ can be denoted as follows:

$$\begin{aligned} H(q_i) &= \mathbb{E}[-\log(p(q_i))], \\ p(q_i) &= \sigma(\text{MLP}_h(q_i'')), \end{aligned} \quad (7)$$

where \mathbb{E} is the expected value operator, $p(q_i)$ denotes the probability of q_i being answered accurately, and σ is the sigmoid function. $H(q_i|e_{i,k})$ can be denoted as follows:

$$\begin{aligned} H(q_i|e_{i,k}) &= \mathbb{E}[-\log(p(q_i, e_{i,k}))], \\ p(q_i, e_{i,k}) &= \sigma(\text{MLP}_h(\text{AP}([q_i'', e_{i,k}']))), \end{aligned} \quad (8)$$

where $p(q_i, e_{i,k})$ is the probability of q_i being answered accurately given $e_{i,k}$, AP denotes the average pooling with kernel size 2. A formal description about this algorithm is shown in Algorithm 1.

Model	Non-diagram T/F	Non-diagram MC	Non-diagram All	Diagram	All
CMR (Zheng et al., 2020)	51.14	30.65	38.72	30.73	34.53
MUTAN (Ben-Younes et al., 2017)	51.72	31.18	39.27	30.29	34.56
MFB (Yu et al., 2017)	51.73	30.65	38.95	30.76	34.65
BAN (Kim et al., 2018)	51.70	31.11	39.22	30.65	34.73
MCAN (Yu et al., 2019)	51.72	32.55	40.10	30.58	35.10
XTQA	58.24	30.33	41.32	32.05	36.46

Table 1: Experimental results (% accuracy) of different-type questions on the validation split. We show the accuracy of True/False (Non-diagram T/F) questions, multiple-choice questions (Non-diagram MC), the whole non-diagram questions (Non-diagram All = Non-diagram T/F \cup Non-diagram MC), multiple-choice diagram questions (Diagram) and total questions (All = Non-diagram \cup Diagram). **Note that all the baselines use the same BERT embeddings and the SimCLR model as XTQA for a fair comparison.**

After generating the top K evidence spans and their representations $e_i'' \in \mathbb{R}^{K \times d_1}$, the learned attention mechanism in Equation 2 is used to obtain the final evidence span representation $e_i''' \in \mathbb{R}^{d_1 \times 1}$.

4.3 Diagram Representation

We use CNNs to obtain the d_2 -dimensional representation $d_i' \in \mathbb{R}^{d_2 \times 1}$ of d_i as follows:

$$d_i' = \text{CNN}_s(d_i). \quad (9)$$

The CNNs could be ResNet (He et al., 2016), SimCLR (Chen et al., 2020) and so on.

4.4 Answer Prediction

After the above modules, we obtain the word-level/global representations q_i'/q_i'' of q_i , the diagram representations d_i' of d_i , the global representations $a_{i,j}''$ of $a_{i,j}$, the evidence span representations e_i''' of e_i and the indexes [START(k), END(k)] of spans.

The mentioned representations are fused to obtain the global fusion feature $g_{i,j} \in \mathbb{R}^{9d_1 \times 1}$ with j -th candidate answer as follows:

$$\begin{aligned} g_{i,j} &= [q_i''; d_i'; a_{i,j}''; e_i'''; g_i^\beta; g_{i,j}^\gamma; g_i^\mu; g_{i,j}^\eta;], \\ g_i^\beta &= \text{BAN}(q_i', d_i'), \quad g_{i,j}^\gamma = W q_i'' \circ W a_{i,j}'', \\ g_i^\mu &= W q_i'' \circ W e_i''', \quad g_{i,j}^\eta = W e_i''' \circ W a_{i,j}'', \\ g_{i,j}^\psi &= W q_i'' \circ W a_{i,j}'' \circ g_i^\beta, \end{aligned} \quad (10)$$

where BAN is the bi-linear attention networks (Kim et al., 2018), $W \in \mathbb{R}^{d_1 \times d_1}$ is the learned weight matrix, $g_i^\beta, g_{i,j}^\gamma, g_i^\mu, g_{i,j}^\eta \in \mathbb{R}^{d_1 \times 1}$ denote the pairwise similarity, and $g_{i,j}^\psi \in \mathbb{R}^{d_1 \times 1}$ is the triple-wise similarity.

To obtain the estimation \hat{a}_i of the correct answer, $g_{i,j}^T$ is projected into a scalar score as follows:

$$\hat{a}_i = \arg \max_{j \in |\mathcal{A}_i|} \text{softmax}(\text{MLP}_c(g_{i,j}^T)). \quad (11)$$

Eventually, not only the answer \hat{a}_i but also the evidence span is provided for students by optimizing the cross-entropy loss function.

5 Experiments

5.1 Datasets and Evaluations

We use the accuracy to evaluate XTQA on the TQA dataset (Kembhavi et al., 2017) that consists of 1,076 lessons with 78,338 sentences and 3,455 diagrams (including very few natural images). The lessons are obtained from the Physical Science, Life Science and Earth Science textbooks of the middle school on-line curricula. The TQA dataset is split into a training set with 666 lessons and 15,154 questions, a validation dataset with 200 lessons and 5,309 questions, and a test set with 210 lessons and 5,797 questions. Among of the total 26,260 questions, 12,567 of them have an accompanying diagram. There are four candidate answers for each diagram question. The non-diagram questions can be classified into two categories: True/False (T/F) with two candidate answers and Multiple Choice (MC) with two to seven candidate answers.

5.2 Implementation Details

In *Question/Answer Representation*, we use BERT (Devlin et al., 2019) to obtain 768-dimensional word embeddings and uni-directional one-layer GRUs with $d_1 = 1024$ hidden units to encode questions and candidate answers. The shared MLPs (FC(1024)-Dropout(0.2)-FC(1)) are used to learn

Model	Non-diagram T/F	Non-diagram MC	Non-diagram All	Diagram	All
BAN (Kim et al., 2018)	48.080	32.96	38.44	27.28	32.11
MFB (Yu et al., 2017)	48.081	31.83	37.72	28.17	32.30
MCAN (Yu et al., 2019)	48.077	33.15	38.56	27.56	32.32
MUTAN (Ben-Younes et al., 2017)	48.075	32.90	38.40	28.29	32.67
CMR (Zheng et al., 2020)	52.022	33.15	39.99	29.54	34.06
Challenge	—	—	42.08	31.75	36.22
XTQA	56.218	33.40	41.67	33.34	36.95

Table 2: Experimental results (% accuracy) of different-type questions on the test split. We show the accuracy of True/False (Non-diagram T/F) questions, multiple-choice questions (Non-diagram MC), the whole non-diagram questions (Non-diagram All = Non-diagram T/F \cup Non-diagram MC), multiple-choice diagram questions (Diagrams) and total questions (All = Non-diagram \cup Diagram). **Note that all the baselines use the same BERT embeddings and the SimCLR model as XTQA for a fair comparison.**

attention coefficients. In *Evidence Span Generation*, the pylucene² is used to conduct paragraphs indexing and searching. The maximum number of paragraphs M , the maximum number of sentences within each paragraph L , the maximum length of each sentence O and the maximum number of evidence span K are set to 1/1, 5/15, 20/15 and 1/1 for non-diagram/diagram question answering respectively. we set the maximum widths of candidate evidence spans to 2. In *Diagram Representation*, we resize the diagrams to 224 owing to the different sizes of them in the TQA dataset. To obtain $d_2 = 2048$ -dimensional diagram representations, we first train the SimCLR³ (Chen et al., 2020) on the diagrams within TQA dataset with default hyper-parameters, and then fine-tune the pre-trained model by the task-specific supervision (TQA). In *Answer Prediction*, the MLPc (FC(2048)-ReLU-Dropout(0.2)-FC(1)) is used to obtain the candidate answer scores.

XTQA is trained by the Adam optimizer with $\beta_1 = 0.9$, $\beta_2 = 0.98$. The base learning rate is $\min(2.5\tau e^{-4}, 1e^{-4})$, where τ is the current epoch. The rate is decayed by 0.1 after 8 epochs. XTQA converges at the end of the 10-th epoch with the batch size 2.

5.3 Baselines

We compare XTQA with several methods that focus on multi-modality fusion as follows⁴:

MFB (Yu et al., 2017) is a multi-modal factorized bi-linear pooling approach. It aims at addressing

²<https://lucene.apache.org/pylucene/>

³We open this code on <https://github.com/keep-smile-001/SimCLR-TQA-master>

⁴All the baselines are implemented in our open source code *openTQA*.

the high dimensionality of the output features and the huge number of parameters caused by the bi-linear pooling based models (Tenenbaum and Freeman, 1997).

MUTAN (Ben-Younes et al., 2017) is a multi-modal tensor-based decomposition approach with a low-rank matrix constraint. It also aims at addressing huge dimensionality issues.

BAN (Kim et al., 2018) is a bi-linear attention network that aims at learning effective interactions between images and questions using the proposed bi-linear attention mechanism.

MCAN (Yu et al., 2019) is a deep modular co-attention network. It aims at obtaining sufficient multi-modality interactions by modularly composing the self-attention of questions and images, as well as the question-guided-attention of images.

CMR (Zheng et al., 2020) is a cross-modality relevance module that can be used in an end-to-end framework. It learns the relevance representations between entities of input modalities and modeling the higher-order relevance between entity relations to perform language and vision reasoning.

Challenge⁵ is a competition of the TQA task. We cite the best results on each type of questions of the test split. The results come from different teams.

5.4 Results

The experimental results on the validation/test split are shown in Table 1/Table 2 respectively.

In Table 1, we can see that XTQA outperforms the best baseline MCAN by 1.36% on the total questions of the validation split. For diagram questions, XTQA outperforms the best baseline MFB by 1.29%. For non-diagram questions, XTQA out-

⁵<https://competitions.codalab.org/competitions/16931#results>

Models	Non-diagram All	Δ	Diagram	Δ	All	Δ
XTQA	41.32		32.05		36.46	
w/o fine-tuning the SimCLR model	41.32	0	30.36	-1.69	35.57	-0.89
w/o the BERT embeddings	41.20	-0.12	29.82	-2.23	35.24	-1.22
w/o fine-grained evidence spans	38.95	-2.37	30.36	-1.69	34.45	-2.01

Table 3: Ablation results (%) accuracy) of the XTQA. Non-diagram All denotes the accuracy on the non-diagram questions. Diagram denotes the accuracy on the diagram questions. All denotes the accuracy on the total questions. Δ denotes the accuracy reduction without the specific module.

performs the best baseline MCAN by 1.22%. For T/F-type questions, XTQA outperforms the best baseline MFB by 6.51%. XTQA performs worst on the MC-type questions, which may be caused by the different data distributions between T/F (two candidate answers) and MC (four to seven candidate answers) questions. Note that all the baselines perform information fusion between top 1 paragraph and questions for non-diagram questions considering the specificity of the TQA task.

In Table 2, we can see that XTQA outperforms the best baseline Challenge by 0.73% on the total questions of the test split. For diagram questions, XTQA outperforms the best baseline Challenge by 1.59%. For non-diagram questions, XTQA underperforms the best baseline Challenge by 0.41%. For TF-type questions, XTQA outperforms the best baseline CMR by 4.196%. All the methods perform poorly on this type of questions except XTQA and CMR, which may be caused by the different data distributions or the difficult questions. For MC-type questions, XTQA outperforms the best baseline MCAN and CMR by 0.25%. Note that XTQA achieves the best performance on the two splits, which shows the effectiveness of our method. In addition, the performance of baselines is different on the two splits, which may be caused by the following reasons. (1) The generation abilities of the baselines are different. (2) The data distribution is different between the validation split and test split. For example, the information of Lesson *earth science and its branches* is mutually exclusive in the two splits.

5.5 Ablation Studies

We perform ablation studies as shown in Table 3 to verify the effectiveness of each module.

The accuracy on the diagram questions drops by 1.69% without fine-tuning the SimCLR model, which shows that fine-tuning the pre-trained model

helps models to learn effective diagram representations to improve the TQA performance.

The accuracy on the non-diagram/diagram questions drop by 0.12% and 2.23% respectively without the BERT embeddings, which shows the significant performance difference of the BERT embeddings on the different task. This phenomenon may be caused by unstable optimizing on the diagram question answering.

The accuracy on the non-diagram/diagram questions drop by 2.37% and 1.69% respectively without fine-grained evidence spans, which shows the effectiveness of our proposed coarse-to-fine grained evidence span generation algorithm.

In short, each component makes its contributions to the performance of the XTQA and our proposed coarse-to-fine grained evidence span generation algorithm plays the biggest role.

5.6 Case Studies

We conduct the case studies as shown in Figure 3 to present the strengths and weaknesses of our method intuitively.

Strengths. XTQA can provide the explicit evidence span for students by the coarse-to-fine grained algorithm. In addition, it can generate evidence spans of different lengths according to the specific question. For example, XTQA provides evidence span of length 1 of the diagram question, and provides evidence span of length 2 of the non-diagram question for students respectively as shown in the middle part of Figure 3.

Weaknesses. If the coarse-grained algorithm makes errors, it will cause the failure to find evidence spans in the fine-grained phase. For example, XTQA finds the wrong top 1 paragraph for the non-diagram question as shown in the middle part of Figure 3, which causes the failure to find the evidence span.

In short, XTQA gives students explainability to

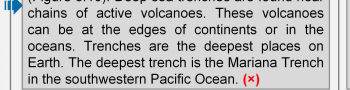
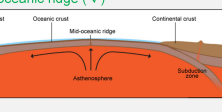
Seafloor Spreading	Coarse-grained Phase	Fine-grained Phase	Questions
<p>Seafloor Bathymetry Before World War II, people thought the seafloor was completely flat and featureless. There was no reason to think otherwise.</p> <p>Echo Sounders But during the war, battleships and submarines carried echo sounders. Their goal was to locate enemy submarines (Figure 6.9). Echo sounders produce sound waves that travel outward in all directions.</p> <p>Features of the Seafloor Scientists were surprised to find huge mountains and deep trenches when they mapped the seafloor. The mid-ocean ridges form majestic mountain ranges through the deep oceans. Deep sea trenches are found near chains of active</p> 	<p>The seafloor spreading hypothesis brought all of these observations together in the early 1960s. Hot mantle material rises up at mid-ocean ridges. The hot magma erupts as lava. The lava cools to form new seafloor. Later, more lava erupts at the ridge. The new lava pushes the seafloor that is at the ridge horizontally away from ridge axis. The seafloor moves! In some places, the oceanic crust comes up to a continent. The moving crust pushes that continent away from the ridge axis as well. If the moving oceanic crust (✓)</p> <p>Scientists were surprised to find huge mountains and deep trenches when they mapped the seafloor. The mid-ocean ridges form majestic mountain ranges through the deep oceans (Figure 6.10). Deep sea trenches are found near chains of active volcanoes. These volcanoes can be at the edges of continents or in the oceans. Trenches are the deepest places on Earth. The deepest trench is the Mariana Trench in the southwestern Pacific Ocean. (✗)</p> 	<p>Hot mantle material rises up at mid-ocean ridges. (✓)</p> <p>Deep sea trenches are found near chains of active volcanoes. These volcanoes can be at the edges of continents or in the oceans.</p>	<p>1. Identify the part of the diagram where hot mantle material rises out of the sea floor A Continental Crust B Oceanic Crust C Subduction Zone D Mid-oceanic ridge (✓)</p>  <p>2. hypothesis explaining how the ocean floor forms A Echo sounder B Mid-ocean ridges (✗) C Abyssal plains D Seafloor spreading E Polar reversal F Magnetometer G Trenches</p>

Figure 3: Case studies to show the strengths and weaknesses of the XTQA. The left part shows the multi-modal context of the Lesson *Seafloor Spreading*. The middle parts show the evidence generation processes by our proposed algorithm. The right part shows the questions of this lesson. These cases come from the validation split.

some extent, and optimizing the coarse-grained algorithm may be the further research direction.

5.7 Discussions

We make an assumption about the evidence generation in Section 1 owing to the lack of supervision. To verify the effectiveness of this assumption, we take some samples that are answered correctly from the test split and manually check whether the generated evidence spans can provide certain explainability for students. The results are show in Figure 4. The accuracy on the non-diagram questions, di-

ent data distributions between splits. For example, the information of Lesson *earth science and its branches* is mutually exclusive in the data splits.

6 Conclusion and Future Work

In this paper, we propose a novel architecture towards span-level eXplanations of the Textbook Question Answering (XTQA). It can provide not only the answers but also the evidences to choose them for students. To generate evidence spans, we propose a coarse-to-fine grained algorithm. In the coarse phase, the algorithm uses the TF-IDF method to find top M paragraphs relevant to questions within the multi-modal context. In the coarse-grained phase, it generates the top K evidence spans by computing the information gain of each candidate evidence span to questions. Experimental results show that XTQA achieves the state-of-the-art performance on the validation split and the test split of the TQA dataset.

In the future, the following directions will be explored: (1) Error reduction of the coarse-grained algorithm may improve the accuracy of evidence span generation. We will explore how to devise an end-to-end architecture to optimize the process of the coarse-grained evidence span generation. (2) External knowledge helps to improve the performance of other tasks such as named entity recognition and visual question answering. An analysis about the TQA dataset (Kembhavi et al., 2017) also shows that about 10% of the questions need external knowledge to answer. We will explore how to integrate the external knowledge into XTQA to improve its performance.

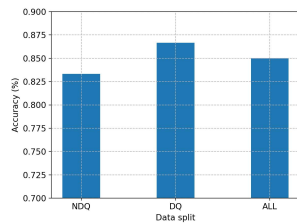


Figure 4: The accuracy of evidence spans on the non-diagram questions (NDQ), diagram questions (DQ), total questions (ALL).

agram questions and total questions are 83.33%, 86.67% and 85% respectively. This shows the evidences for most of the questions answered correctly provide explainability for students and proves the validity of our assumption to some extent.

In addition, we find XTQA and other baselines have poor generalization abilities on the validation split and the test split, which may be caused by the following reasons. (1) Small datasets may easily lead to overfitting. (2) There may exist differ-

References

Peter Anderson, Xiaodong He, Chris Buehler, Damien Teney, Mark Johnson, Stephen Gould, and Lei Zhang. 2018. Bottom-up and top-down attention for image captioning and visual question answering. In *Proceedings of the IEEE conference on computer vision and pattern recognition*, pages 6077–6086.

Stanislaw Antol, Aishwarya Agrawal, Jiasen Lu, Margaret Mitchell, Dhruv Batra, C Lawrence Zitnick, and Devi Parikh. 2015. Vqa: Visual question answering. In *Proceedings of the IEEE international conference on computer vision*, pages 2425–2433.

Hedi Ben-Younes, Rémi Cadene, Matthieu Cord, and Nicolas Thome. 2017. Mutan: Multimodal tucker fusion for visual question answering. In *Proceedings of the IEEE international conference on computer vision*, pages 2612–2620.

Ting Chen, Simon Kornblith, Mohammad Norouzi, and Geoffrey Hinton. 2020. A simple framework for contrastive learning of visual representations. *arXiv preprint arXiv:2002.05709*.

Jacob Devlin, Ming-Wei Chang, Kenton Lee, and Kristina Toutanova. 2019. Bert: Pre-training of deep bidirectional transformers for language understanding. In *Proceedings of the 2019 Conference of the North American Chapter of the Association for Computational Linguistics: Human Language Technologies, Volume 1 (Long and Short Papers)*, pages 4171–4186.

Ming Ding, Chang Zhou, Qibin Chen, Hongxia Yang, and Jie Tang. 2019. Cognitive graph for multi-hop reading comprehension at scale. In *Proceedings of the 57th Annual Meeting of the Association for Computational Linguistics*, pages 2694–2703.

Peng Gao, Haoxuan You, Zhanpeng Zhang, Xiaogang Wang, and Hongsheng Li. 2019. Multi-modality latent interaction network for visual question answering. In *Proceedings of the IEEE International Conference on Computer Vision*, pages 5825–5835.

Kaiming He, Xiangyu Zhang, Shaoqing Ren, and Jian Sun. 2016. Deep residual learning for image recognition. In *Proceedings of the IEEE conference on computer vision and pattern recognition*, pages 770–778.

Aniruddha Kembhavi, Minjoon Seo, Dustin Schwenk, Jonghyun Choi, Ali Farhadi, and Hannaneh Hajishirzi. 2017. Are you smarter than a sixth grader? textbook question answering for multimodal machine comprehension. In *Proceedings of the IEEE Conference on Computer Vision and Pattern Recognition*, pages 4999–5007.

Mahmoud Khademi. 2020. Multimodal neural graph memory networks for visual question answering. In *Proceedings of the 58th Annual Meeting of the Association for Computational Linguistics*, pages 7177–7188.

Jin-Hwa Kim, Jaehyun Jun, and Byoung-Tak Zhang. 2018. Bilinear attention networks. In *Advances in Neural Information Processing Systems*, pages 1564–1574.

Jin-Hwa Kim, Kyoung Woon On, Woosang Lim, Jeonghee Kim, Jung-Woo Ha, and Byoung-Tak Zhang. 2017. Hadamard product for low-rank bilinear pooling. In *5th International Conference on Learning Representations*.

Jinhyuk Lee, Seongjun Yun, Hyunjae Kim, Miyoung Ko, and Jaewoo Kang. 2018. Ranking paragraphs for improving answer recall in open-domain question answering. In *Proceedings of the 2018 Conference on Empirical Methods in Natural Language Processing*, pages 565–569.

Wendy Grace Lehnert. 1977. *The process of question answering*. Ph.D. thesis, Yale University.

Jie Ma, Jun Liu, Yufei Li, Xin Hu, Yudai Pan, Shen Sun, and Qika Lin. 2020. Jointly optimized neural coreference resolution with mutual attention. In *Proceedings of the 13th International Conference on Web Search and Data Mining*, pages 402–410.

Jiayuan Mao, Chuang Gan, Pushmeet Kohli, Joshua B Tenenbaum, and Jiajun Wu. 2019. The neuro-symbolic concept learner: Interpreting scenes, words, and sentences from natural supervision. In *International Conference on Learning Representations*.

Yixin Nie, Songhe Wang, and Mohit Bansal. 2019. Revealing the importance of semantic retrieval for machine reading at scale. In *Proceedings of the 2019 Conference on Empirical Methods in Natural Language Processing and the 9th International Joint Conference on Natural Language Processing*, pages 2553–2566.

Apoorv Saxena, Aditay Tripathi, and Partha Talukdar. 2020. Improving multi-hop question answering over knowledge graphs using knowledge base embeddings. In *Proceedings of the 58th Annual Meeting of the Association for Computational Linguistics*, pages 4498–4507.

Joshua B Tenenbaum and William T Freeman. 1997. Separating style and content. In *Advances in neural information processing systems*, pages 662–668.

Wei Wang, Ming Yan, and Chen Wu. 2018. Multi-granularity hierarchical attention fusion networks for reading comprehension and question answering. In *Proceedings of the 56th Annual Meeting of the Association for Computational Linguistics (Volume 1: Long Papers)*, pages 1705–1714.

Zichao Yang, Xiaodong He, Jianfeng Gao, Li Deng, and Alex Smola. 2016. Stacked attention networks for image question answering. In *Proceedings of the IEEE conference on computer vision and pattern recognition*, pages 21–29.

Kexin Yi, Jiajun Wu, Chuang Gan, Antonio Torralba, Pushmeet Kohli, and Josh Tenenbaum. 2018. Neural-symbolic vqa: Disentangling reasoning from vision and language understanding. In *Advances in neural information processing systems*, pages 1031–1042.

Zhou Yu, Jun Yu, Yuhao Cui, Dacheng Tao, and Qi Tian. 2019. Deep modular co-attention networks for visual question answering. In *Proceedings of the IEEE conference on computer vision and pattern recognition*, pages 6281–6290.

Zhou Yu, Jun Yu, Jianping Fan, and Dacheng Tao. 2017. Multi-modal factorized bilinear pooling with co-attention learning for visual question answering. In *Proceedings of the IEEE international conference on computer vision*, pages 1821–1830.

Chen Zheng, Quan Guo, and Parisa Kordjamshidi. 2020. Cross-modality relevance for reasoning on language and vision. In *Proceedings of the 58th Annual Meeting of the Association for Computational Linguistics*, pages 7642–7651. Association for Computational Linguistics.